Supporting Information

Effect of Pd(II) Uptake on High-Temperature Phase Transitions in a Hybrid Organic-Inorganic Perovskite Semiconductor

Yan Xu, Ke Xu, Lei He, Jie Mu, Ti-Jian Yin, Jin-Tao Men and Qiong Ye*

Characterizations and Methods

Phase Purity. The powder X-ray diffraction (PXRD) analysis of **1** and **1-Pd** were performed on Rigaku Ultima IV multipurpose X-ray Diffractometer at 293 K. The diffraction pattern is obtained in the range of 2θ (5 ~ 50°) with a step size of 0.02°.

Single-Crystal X-ray Diffraction (SCXRD). The single-crystal X-ray diffraction of **1** at 300, 377 and 416 K were obtained on Rigaku Saturn 924 diffractometer with Mo Kα radiation (λ = 0.71073 Å). The data were processed with the CrystalClear software package. The structures of **1** were solved by direct methods and refined with the SHELXTL software package which used full-matrix least-squares methods based on F^2 data. The anisotropic refinement of all non-H atoms was performed, and the positions of all H atoms were geometrically generated. The crystallographic data and the details of structure refinement are listed in **Table S1**.

DSC Measurements. Differential scanning calorimetry (DSC) of **1** and **1-Pd** were measured on PerkinElmer Diamond DSC instrument that 15.2 mg (**1**) and 12.4 mg (**1-Pd**) powder samples were placed in aluminum crucibles with heating and cooling rates of 20 K/min under nitrogen atmosphere.

Dielectric Measurements. The dielectric responses of **1** and **1-Pd** were performed on Tonghui Model TH2828A impedance analyzer. The powder-pressed pellets of about 2-3 mm pasted with silver or carbon conducting glue were used in dielectric

measurements. The temperature-dependent dielectric constants were measured on a Tonghui Model TH2828A impedance analyzer at the frequencies of 1 MHz, with an applied ac voltage at 1 V. During the experiment, the heating process is completed by heating furnace, and the cooling is completed by liquid nitrogen.

Ultraviolet–visible (UV-vis) Absorption Spectrum. At room temperature, the UV–vis diffuse reflectance spectrum of **1** was measured on Shimadzu (Tokyo, Japan) UV–2600 spectrophotometer. $BaSO_4$ was selected as the standard (100%) reflectivity reference.

Elemental Analysis. For the elemental analysis, the regular elemental analysis was determined with Elementar vario EL III instrument. Inductively coupled plasma (ICP) elemental analysis was performed on Spectroblue ICP-OES.

Conductivity Measurements

At different pressures, the electrical conductivity of compounds **1** and **1-Pd** were measured on a four-terminal powder resistivity tester at room temperature.

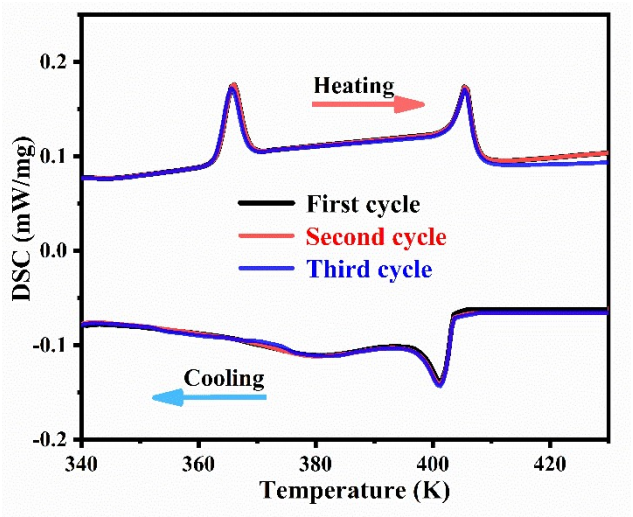

Figure S1. DSC curves of compound **1** during multiple rounds of heating and cooling.

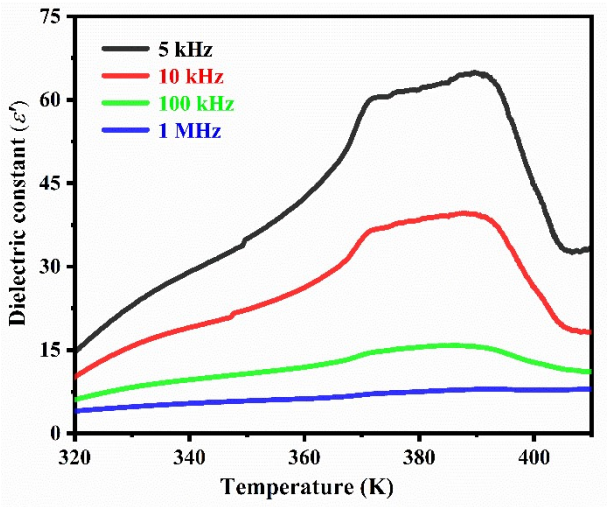

Figure S2. Temperature dependence of the real part (ε′) of compound **1** during the heating at different frequencies.

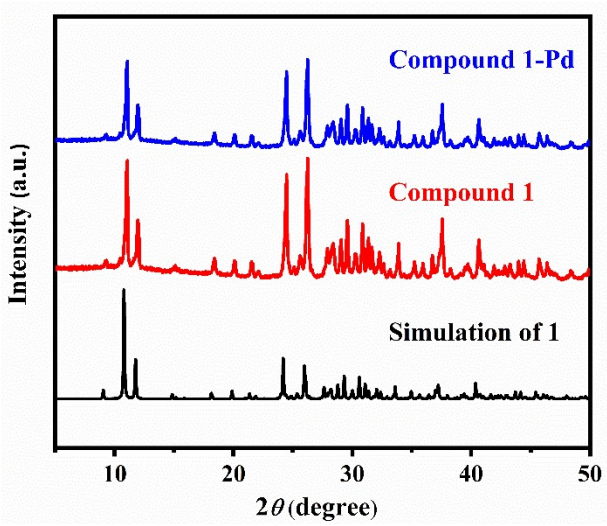

Figure S3. The powder X-ray diffraction patterns of compounds **1** and **1-Pd** at 293 K.

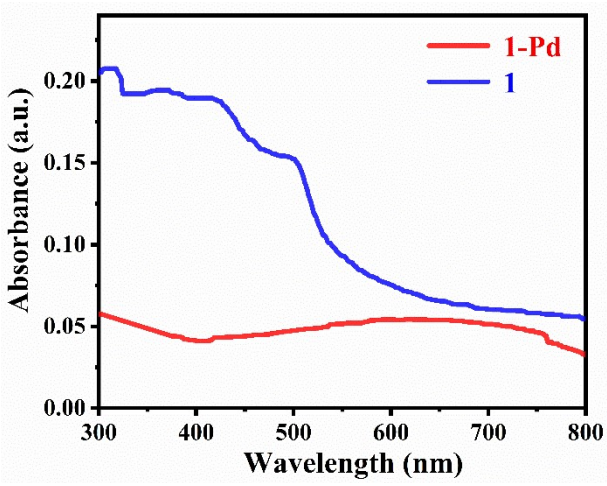

Figure S4. UV-vis absorption spectrum for **1** and **1-Pd.**

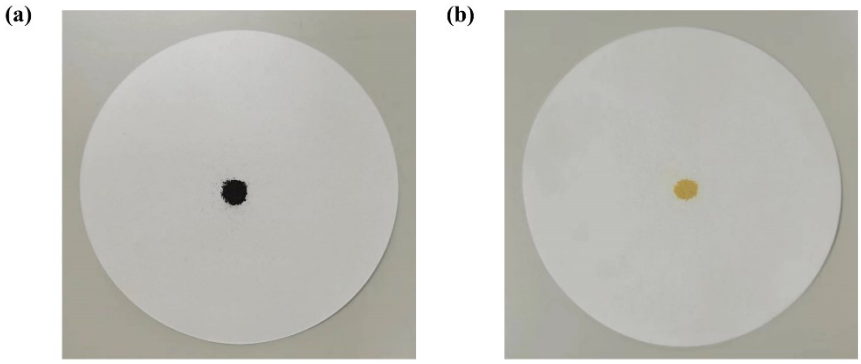

Figure S5. Comparison graphs before and after desorption: (a) before desorption; (b) after desorption.

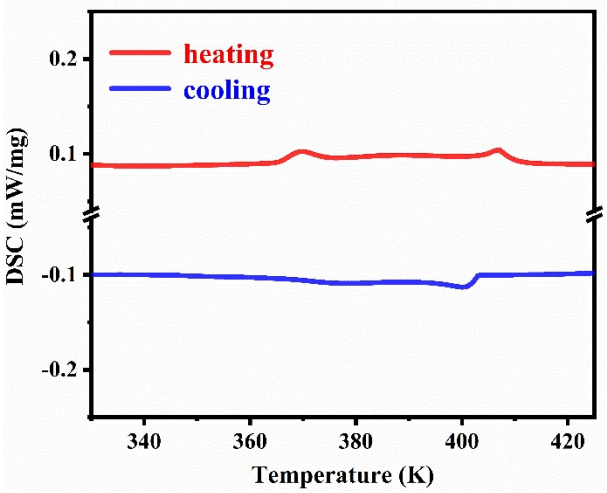

Figure S6. DSC curves of the powder after desorption during the cooling and heating cycles.

Table S1. Crystal data and structure refinement details of **1**.

Chemical Formula		$[C_3H_7N_2S]PbI_3$	
T (K)	300 K	377 K	416 K
Formula weight	691.06	691.06	1382.13
Crystal system	Orthorhombic	Orthorhombic	Orthorhombic
Space group	*Pbca*	*Pmcn*	*Cmcm*
a/Å	15.0602 (7)	8.7522 (15)	8.9920 (14)
b/Å	8.3101 (3)	17.620 (2)	17.951 (4)
c/Å	19.5118 (8)	8.2301 (11)	8.1262 (11)
α(deg)	90	90	90
β(deg)	90	90	90
γ(deg)	90	90	90
V/Å^3	2441.94 (18)	1269.2 (3)	1311.7 (4)
Z	8	4	2
F (000)	2368.0	1184.0	1184.0
GOF	0.977	1.0120	1.093
R_1	0.0664 (2336)	0.0803	0.0872 (374)
wR_2	0.1830 (3156)	0.1844	0.2945 (567)

Table S2. After a complete round of structural transitions of compound **1**, the structure of **1** after returning to room temperature is the same as the structure at room temperature at the beginning.

T (K)	*a*/Å	*b*/Å	*c*/Å	*V*/Å^3	Space group	Space group number
300 K	15.0602	8.3101	19.5118	2441.94(18)	*Pbca*	61
377 K	8.2363	8.7565	17.6090	1269.98(19)	*Pnma*	62
416 K	8.9920	17.9510	8.1262	1311.70(4)	*Cmcm*	63
395 K	8.1651	8.8332	17.8750	1289.20(2)	*Pnma*	62
390 K	8.1862	8.8032	17.8050	1283.10(2)	*Pnma*	62

385 K	8.2042	8.7954	17.7423	1280.30(3)	*Pnma*	62
380 K	8.2237	8.7698	17.6353	1271.90(2)	*Pnma*	62
375 K	8.2362	8.7467	17.6096	1268.59(19)	*Pnma*	62
370 K	8.2450	8.7228	17.5483	1262.05(18)	*Pnma*	62
300 K	15.0824	8.3078	19.5158	2445.40(2)	*Pbca*	61

Table S3. The bond lengths and angles at 300 K.

Bond lengths (Å)		**Bond angles (°)**	
Pb1—I1	3.1703 (8)	I1—Pb1—I1^{i}	92.43 (3)
Pb1—I1^{i}	3.2429 (8)	I1^{i}—Pb1—I2^{i}	84.14 (2)
Pb1—I2^{i}	3.3049 (8)	I1—Pb1—I2	86.80 (2)
Pb1—I2	3.2154 (8)	I1—Pb1—I2^{i}	106.21 (2)
Pb1—I3	3.2323 (8)	I1—Pb1—I3	86.72 (2)
Pb1—I3^{i}	3.3042 (8)	I1—Pb1—I3^{i}	174.77 (3)
S1—C3	1.799 (14)	I1^{i}—Pb1—I3^{i}	84.35 (2)
S1—C1	1.694 (14)	I2—Pb1—I1^{i}	104.25 (2)
N2—C1	1.295 (16)	I2—Pb1—I2^{i}	164.41 (4)
N2—C2	1.44 (2)	I2—Pb1—I3^{i}	89.99 (2)
C3—C2	1.468 (19)	I2—Pb1—I3	79.94 (2)
C1—N1	1.331 (13)	I3—Pb1—I1^{i}	175.68 (3)
		I3—Pb1—I2^{i}	92.02 (2)
		I3^{i}—Pb1—I2^{i}	77.62 (2)
		I3—Pb1—I3^{i}	96.79 (3)
		Pb1—I1—Pb1^{ii}	80.761 (19)
		Pb1—I2—Pb1^{ii}	79.167 (18)
		Pb1—I3—Pb1^{ii}	78.937 (19)
		C1—S1—C3	91.4 (5)
		C1—N2—C2	115.3 (12)
		C2—C3—S1	108.1 (10)

		N2—C1—S1	115.5 (9)
		N2—C1—N1	123.8 (14)
		N1—C1—S1	120.7 (11)
		N2—C2—C3	109.7 (12)

Table S4. The bond lengths and angles at 377 K.

Bond lengths (Å)		**Bond angles (°)**	
Pb1—I1^{i}	3.2479 (13)	I1—Pb1—I1^{i}	80.47 (5)
Pb1—I1^{ii}	3.2606 (13)	I1^{iii}—Pb1—I1^{i}	179.14 (3)
Pb1—I1	3.2479 (13)	I1—Pb1—I1^{ii}	179.14 (3)
Pb1—I1^{iii}	3.2606 (13)	I1^{iii}—Pb1—I1^{ii}	80.09 (5)
Pb1—I2	3.1851 (16)	I2^{ii}—Pb1—I1^{i}	94.01 (3)
Pb1—I2^{ii}	3.2449 (16)	I2—Pb1—I1^{ii}	94.52 (3)
S1—C3	1.74 (3)	I2—Pb1—I1^{iii}	94.52 (3)
S1—C1	1.70 (4)	I2^{ii}—Pb1—I1^{ii}	85.14 (3)
C3—C2	1.45 (4)	I2^{ii}—Pb1—I1	94.01 (3)
N2—C2	1.35 (4)	I2—Pb1—I1^{i}	86.32 (3)
N2—C1	1.38 (4)	I2^{ii}—Pb1—I1^{iii}	85.14 (3)
		I2—Pb1—I1	86.32 (3)
		C1—S1—C3	90.3 (13)
		C1—N2—C2	108 (3)
		N2—C2—C3	117 (3)
		C2—C3—S1	107 (2)
		N2—C1—S1	117 (2)
		N1—C1—S1	115 (2)
		N1—C1—N2	128 (3)

Table S5. The bond lengths and angles at 416 K.

Bond lengths (Å)		Bond angles (º)	
Pb1—I1	3.247 (2)	I2—Pb1—I1	85.20 (7)
Pb1—I1^{i}	3.247 (2)	I2^{ii}—Pb1—I1	94.80 (7)
Pb1—I1^{ii}	3.247 (2)	I2^{ii}—Pb1—I2	180
Pb1—I1^{iii}	3.247 (2)	C1—S1—C3	101.5 (6)
Pb1—I2^{ii}	3.205 (3)	C1—N2—H2	124.1
Pb1—I2	3.205 (3)	C1—N2—C2	111.7 (8)
S1—C1	1.5777 (11)	C2—N2—H2	124.1
S1—C3	1.5780 (11)	N2—C1—S1	107.5 (7)
N2—C1	1.394 (10)	N1—C1—S1	125 (2)
N2—C2	1.410 (10)	N1—C1—N2	128 (2)
C1—N1	1.298 (10)	C2—C3—S1	107.5 (7)
C3—C2	1.394 (10)	C3—C2—N2	111.8 (8)

Table S6. The torsion angles [°] for **1** at 300 K.

Bond angles (º)	**300 K**
S1—C3—C2—N2	3.5 (19)
C3—S1—C1—N2	0.0 (14)
C3—S1—C1—N1	−176.9 (15)
C1—S1—C3—C2	−2.1 (13)
C1—N2—C2—C3	−4 (2)
C2—N2—C1—S1	2 (2)
C2—N2—C1—N1	179.0 (17)

Table S7. The torsion angles [°] for **1** at 377 K.

Bond angles (º)	**377 K**

S1—C3—C2—N2	−0.0
S1—C1—N2—C2	−0.0
C3—C2—N2—C1	0.0

Table S8. The torsion angles [°] for **1** at 416 K.

Bond angles (º)	**416 K**
S1—C3—C2—N2	0.00 (3)
C1—S1—C3—C2	0.000 (17)
C1—N2—C2—C3	0.00 (3)
C3—S1—C1—N2	0.000 (13)
C3—S1—C1—N1	180.00 (2)
C2—N2—C1—S1	0.00 (3)
C2—N2—C1—N1	180.00 (3)